Article

Unexpected Relative Aqueous Solubilities of a Phosphotyrosine Analogue and Two Phosphonate Derivatives

Stefan Boresch, Martin Leitgeb, Aleksandra Beselman, and Alexander D. MacKerell

J. Am. Chem. Soc., **2005**, 127 (13), 4640-4648• DOI: 10.1021/ja044935h • Publication Date (Web): 10 March 2005

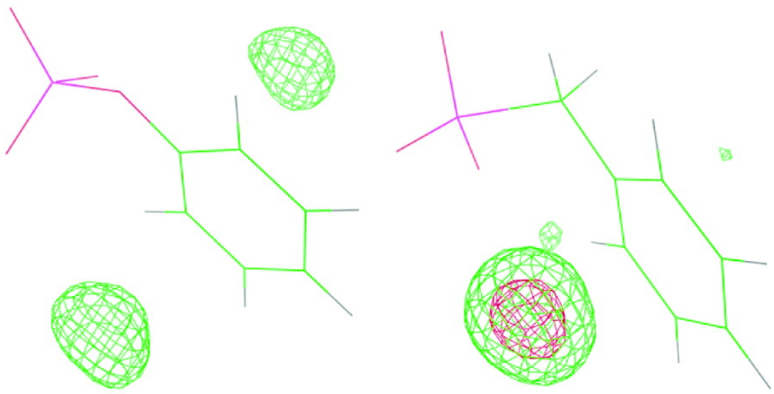

J|A|C|S
ARTICLES
Published on Web 03/10/2005

Unexpected Relative Aqueous Solubilities of a Phosphotyrosine Analogue and Two Phosphonate Derivatives

Stefan Boresch,*,† Martin Leitgeb,† Aleksandra Beselman,‡ and Alexander D. MacKerell, Jr.*,‡

Contribution from the Biomolecular Simulation Group, Institut für Biomolekulare Strukturchemie, Universität Wien, Währingerstraβe 17, 1090 Wien, Austria, and Department of Pharmaceutical Sciences, School of Pharmacy, University of Maryland, Baltimore, 20 Penn Street, Baltimore, Maryland 21201

Received August 21, 2004; E-mail: stefan@mdy.univie.ac.at; alex@outerbanks.umaryland.edu

Abstract: Phosphotyrosine (pTyr) is an essential component of biological signaling, often being a determinant of protein−protein interactions. Accordingly, a number of drug discovery efforts targeting signal transduction pathways have included phosphotyrosine and analogues as essential components of the lead compounds. Toward the goal of improved biological efficacy, the phosphonate and difluoro phosphonate analogues of pTyr have been employed in inhibitor design because of their stability to hydrolysis and enhanced binding affinity in certain cases. To quantitate the contribution of aqueous solubility of pTyr, phosphonomethyl phenylalanine (Pmp), and difluorophosphonomethyl phenylalanine (F_2Pmp) to their relative binding affinities, free energy perturbation calculations were undertaken on the mimetics phenol phosphate (PP), benzyl phosphonate (BP), and difluorobenzyl phosphonate (F_2BP), including development of empirical force field parameters compatible with the CHARMM all-atom force fields. Notably, it is shown that the most favorably solvated compound of the series is BP, followed by PP, with F_2BP the least favorably solvated for both the mono- and dianionic forms of the compounds. The molecular origin of this ordering is shown to be due to changes in charge distribution, in the comparatively larger size of the fluorine atoms, as well as in differences of local solvation between PP and BP. The implications of the differences in aqueous solubility toward the relative binding potencies of pTyr-, Pmp-, and F_2Pmp-containing peptide ligands are discussed. Our results indicate that one general principle explaining the efficacy of selective fluorination to enhance binding affinities may lie in the ability of fluorine atoms to increase the hydrophobicity of a ligand while maintaining its capability to form hydrogen bonds.

1. Introduction

Tyrosine phosphate plays an essential role in signal transduction due to its ability to facilitate specific protein−protein interactions. Signaling pathways involving phosphotyrosine(s) (pTyr) regulate numerous cell functions including mitogenesis, growth, cell−cell interactions, gene transcription, metabolism, and the immune response.[1] Disruptions of these pathways have been implicated in several diseases, making several of the proteins involved high-profile drug targets.[1,2] While initially the process of pTyr creation by protein tyrosine kinases (PTK) was thought to be the central step in pTyr-dependent signaling, the importance of dephosphorylation by protein tyrosine phosphatases (PTP) is now well-established.[1] In addition, a variety of proteins that contain SH2, phosphotyrosine binding (PTB), or other pTyr binding domains share the pTyr moiety as an essential component of protein−substrate interactions. Much of the work to elucidate the mechanistic role in signaling of PTPs and proteins containing pTyr binding domains is concerned with the development of tight binding pTyr analogues.[3]

The phenyl phosphate moiety of pTyr has been the focal point of inhibitor development for several reasons. First, as alluded to above, its presence makes a significant contribution to the binding of peptides to their target proteins. Second, the phosphodiester linkage is labile, and its hydrolysis needs to be prevented. Third, the 2-fold negative charge of the pTyr moiety can hinder bioavailability. These latter two points are particularly relevant to drug-related inhibitor development, motivating efforts to provide nonpeptidic lead compounds that include pTyr or analogues.[4−6] Finally, since there are substantial differences in the binding modes of pTyr to SH2 domains, PTB domains, and PTPs, tyrosyl phosphate is an obvious starting point to achieve selectivity in inhibitors targeting these receptor types.[3]

† Universität Wien.
‡ University of Maryland.

(1) Hunter, T. *Cell* **1995**, *80*, 225−236.
(2) Hunter, T. *Cell* **2000**, *100*, 113−127.
(3) Burke, T. R., Jr.; Yao, Z. J.; Liu, D. G.; Voigt, J.; Gao, Y. *Biopolymers* **2001**, *60*, 32−44.
(4) Burke, T. R., Jr.; Zhang, Z.-Y. *Biopolymers* **1998**, *47*, 225−241.
(5) Jia, Z.; Ye, Q.; Dinaut, A. N.; Wang, Q.; Waddleton, D.; Payette, P.; Ramachandran, C.; Kennedy, B.; Hum, G.; Taylor, S. D. *J. Med. Chem.* **2001**, *44*, 4584−4594.
(6) Leung, C.; Grzyb, J.; Lee, J.; Meyer, N.; Hum, G.; Jia, C.; Liu, S.; Taylor, S. D. *Bioorg. Med. Chem.* **2002**, *10*, 2309−2323.

10.1021/ja044935h CCC: $30.25

One of the first modifications of pTyr motivated by inhibitor development was the introduction of a phosphonate group; that is, the exchange of the phosphate ester oxygen by the non-hydrolyzable CH_2 group. While phosphonomethyl phenylalanine (Pmp) binds to both PTP and SH2 domains, the binding affinities are significantly reduced relative to parent phosphotyrosine-containing peptides. For PTPs and most SH2 domains these poor binding properties could be remedied by introducing fluorine atoms onto the Pmp methylene bridge;[4,7] that is, by replacing Pmp with difluorophosphonomethyl phenylalanine (F_2Pmp). Fluorine substitution is generally known to enhance a drug's selectivity,[8] although decreases in affinity upon fluorination have been observed.[9] Fluorination also provides protective effects against physiological metabolism.[10] Taking advantage of these characteristics, several peptidic and non-peptide PTP inhibitors that include fluorinated groups other than F_2Pmp were developed.[5,6,11] For example, fluoro-*O*-malonyltyrosine exhibited a 10-fold enhancement in potency toward PTP compared with the *O*-malonate itself.[11]

One particularly striking example of the impact of fluorination on ligand binding is the replacement of Pmp in the hexapeptide DADE−Pmp−YL by F_2Pmp. Introducing the difluoromethyl moiety increased the binding affinity 1000-fold toward PTP1.[12] The F_2Pmp-containing peptide also binds 100 times more tightly than the pTyr-containing peptide.[13] Although the series pTyr, Pmp, F_2Pmp has been well-characterized at the biochemical level, an atomic-detail understanding of the effects of the fluorination on the binding affinity has yet to be obtained. The issue is complicated further by the fact that the degree to which the affinity is affected depends on the receptor protein. For example, in contrast to PTPs, F_2Pmp enhances binding affinities toward many SH2 domains only marginally, if at all.[14−16] These experimental observations combined with our lack of a detailed understanding of the determinants of the impact of fluorination on binding affinity motivated the present study.

The tools of computational chemistry are ideally suited to help investigate problems of this kind. In addition to the ability to relate structural information to a detailed energetic analysis at atomic resolution, they also make it possible to address questions outside the scope of normal biochemical studies. With respect to the binding properties of pTyr, Pmp, and F_2Pmp, all analyses to date have focused on the protein−ligand complex. However, it is also possible that differences in the aqueous solubilities of the ligands affect the binding affinity,[17] something that is straightforward to investigate by computer simulation.[18] A prerequisite for detailed computational studies is the availability of high-quality force field parameters for the fluorinated compounds that are balanced with respect to the water and protein force fields being used. Recently, parameters for fluoroethanes that are compatible with the CHARMM22 and CHARMM27 force fields[19,20] were developed.[21] Parameters for pTyr have been available for CHARMM for quite some time.[22] In this work, we extend the work by Feng and co-workers[22] and present parameters for the pTyr mimetics Pmp and F_2Pmp. These parameters are then used to compute the solvation free energy differences between phenol phosphate (PP), benzyl phosphonate (BP), and difluorobenzyl phosphonate (F_2BP), which are the corresponding side chain analogues of pTyr, Pmp, and F_2Pmp.

The remainder of this article is organized as follows. Methodological details of the free energy simulations are given in section 2. In section 3.1 we summarize the parametrization process. The full details of the parameter optimization approach, including a complete parameter listing, are included in the Supporting Information. The results of the free energy simulations and of additional molecular dynamics (MD) simulations are presented in section 3.2. In the concluding Discussion section we address the potential implications of our results with respect to understanding the observed binding affinities of Pmp- and F_2Pmp-containing peptides toward PTPs and SH2 domains.

2. Methods

The relative solvation free energies between PP, BP, and F_2BP were computed by thermodynamic integration (TI) free energy calculations.[18] All simulations described below were carried out using the biomolecular simulation program CHARMM;[23] its PERT module was used for the free energy simulations. Methodological details concerning the parametrization are given in the Supporting Information.

We studied both the dianionic and monoanionic forms of the three phosphate/phosphonate moieties (see Figure 1). Calculations were always carried out for identical charge states; that is, we did not compute the free energy difference of protonation (e.g., $PP^{-2} \rightarrow PP^{-1}$). On the basis of the experimental evidence by Chen et al.,[12] the protonation state of the ligands has no effect on the binding affinities, and thus, the dianions are of primary interest. If, however, it were found that the solvation free energy differences might have a bearing on the observed binding affinities, then it is of some interest whether the same ranking of solvation free energies is obtained in the monoanionic and in the dianionic states.

The usual thermodynamic cycle[24] was employed to determine the (relative) free energy differences of solvation $\Delta\Delta A_{solv}$; it is shown below

(7) Burke, T. R., Jr.; Smyth, M.; Nomizu, M.; Otaka, A.; Roller, P. P. *J. Org. Chem.* **1993**, *58*, 1336−1340.
(8) Clark, M. T.; Adejare, A.; Shams, G.; Feller, D. R.; Miller, D. D. *J. Med. Chem.* **1987**, *30*, 86−90.
(9) Markovich, K. M.; Tantishaiyakul, V.; Hamada, A.; Miller, D. D.; Romstedt, K. J.; Shams, G.; Shin, Y.; Fraundorfer, P. F.; Doyle, K.; Feller, D. R. *J. Med. Chem.* **1992**, *35*, 466−479.
(10) O'Neill, P. M.; Harrison, A. C.; Storr, R. C.; Hawley, S. R.; Ward, S. A.; Park, B. K. *J. Med. Chem.* **1994**, *37*, 1362−1370.
(11) Burke, T. R., Jr.; Ye, B.; Akamatsu, M.; Ford, H., Jr.; Yan, X.; Kole, H. K.; Wolf, G.; Shoelson, S. E.; Roller, P. P. *J. Med. Chem.* **1996**, *39*, 1021−1027.
(12) Chen, L.; Wu, L.; Otaka, A.; Smyth, M. S.; Roller, P. P.; Burke, T. R., Jr.; den Hertog, J.; Zhang, Z.-Y. *Biochem. Biophys. Res. Commun.* **1995**, *216*, 976−984.
(13) Burke, T. R., Jr.; Kole, H. K.; Roller, P. P. *Biochem. Biophys. Res. Commun.* **1994**, *204*, 129−134.
(14) Burke, T. R., Jr.; Smyth, M. S.; Otaka, A.; Nomizu, M.; Roller, P. P.; Wolf, G.; Case, R.; Shoelson, S. E. *Biochemistry* **1994**, *33*, 6490−6494.
(15) Charifson, P. S.; Shewchuk, L. M.; Rocque, W.; Hummel, C. W.; Jordan, S. R.; Mohr, C.; Pacofsky, G. J.; Peel, M. R.; Rodriguez, M.; Sternbach, D. D.; Consler, T. G. *Biochemistry* **1997**, *36*, 6283−6293.
(16) Yao, Z. J.; King, C. R.; Cao, T.; Kelley, J.; Milne, G. W. A.; Burke, T. R., Jr. *J. Med. Chem.* **1999**, *42*, 25−35.
(17) Lieske, S. F.; Yang, B.; Eldefrawi, M. E.; MacKerell, A. D., Jr.; Wright, J. *J. Med. Chem.* **1998**, *41*, 864−876.
(18) Straatsma, T. P. Free Energy by Molecular Simulation. In *Reviews in Computational Chemistry*; Lipkowitz, K. B., Boyd, D. B., Eds.; VCH: New York, 1996; Vol. 9.
(19) MacKerell, A. D., Jr.; Wiorkiewicz, J. K.; Karplus, M. *J. Am. Chem. Soc.* **1995**, *117*, 11946−11975.
(20) MacKerell, A. D., Jr.; Bashford, D.; Bellott, M.; Dunbrack, R. L., Jr.; Evanseck, J. D.; Field, M. J.; Fischer, S.; Gao, J.; Guo, H.; Ha, S.; Joseph-McCarthy, D.; Kuchnir, L.; Kuczera, K.; Lau, F. T. K.; Mattos, C.; Michnick, S.; Ngo, T.; Nguyen, D. T.; Prodhom, B.; Reiher, W. E., III; Roux, B.; Schlenkrich, M.; Smith, J.; Stote, R.; Straub, J.; Watanabe, M.; Wiorkiewicz-Kuczera, J.; Yin, D.; Karplus, M. *J. Phys. Chem. B* **1998**, *102*, 3586−3616.
(21) Chen, I. J.; Yin, D.; MacKerell, A. D., Jr.; *J. Comput. Chem.* **2002**, *23*, 199−213.
(22) Feng, M.-H.; Philippopoulos, M.; MacKerell, A. D., Jr.; Lim, C. *J. Am. Chem. Soc.* **1996**, *118*, 11265−11277.
(23) Brooks, B. R.; Bruccoleri, R. E.; Olafson, B. D.; States, D. J.; Swaminathan, S.; Karplus, M. *J. Comput. Chem.* **1983**, *4*, 187−217.
(24) Tembe, B. L.; McCammon, J. A. *Comput. Chem.* **1984**, *8*, 281−283.

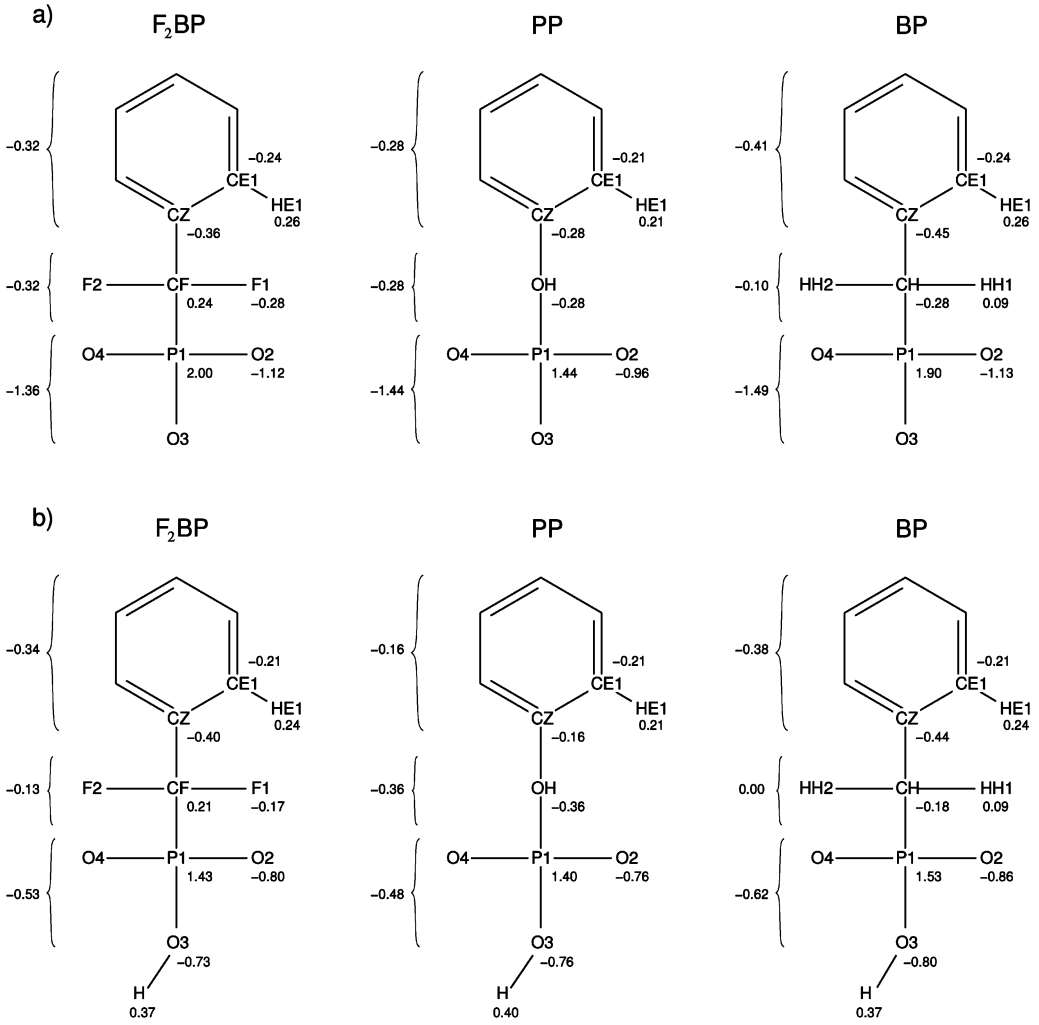

Figure 1. Dianionic (a) and monoanionic (b) forms of the three solutes studied: F_2BP, PP, and BP. Relevant partial charges and atom labels are shown as well.

for the solvation free energy difference between PP and BP.

$$\begin{array}{ccc} (\mathrm{PP})_g & \xrightarrow{\Delta A_{gas}} & (\mathrm{BP})_g \\ \downarrow \Delta A^{PP}_{solv} & & \downarrow \Delta A^{BP}_{solv} \\ (\mathrm{PP})_{aq} & \xrightarrow{\Delta A_{sol}} & (\mathrm{BP})_{aq} \end{array} \qquad (1)$$

We computed the free energy differences for the alchemical transmutations (e.g., between PP and BP) in the gas phase (subscript g, ΔA_{gas}) and in aqueous solution (subscript aq, ΔA_{sol}), from which one obtains[18,24]

$$\Delta\Delta A^{PP\rightarrow BP}_{solv} = \Delta A^{PP\rightarrow BP}_{sol} - \Delta A^{PP\rightarrow BP}_{gas} \qquad (2)$$

For a given charge state (monoanionic, dianionic), we computed all three possible solvation free energy differences, i.e., $\Delta\Delta A^{PP\rightarrow BP}_{solv}$, $\Delta\Delta A^{BP\rightarrow F_2BP}_{solv}$, and $\Delta\Delta A^{F_2BP\rightarrow PP}_{solv}$. Clearly, the sum of these three free energy differences has to be zero; applying this cycle closure criterion individually to the results in the gas phase (ΔA_{gas}), in aqueous solution (ΔA_{sol}), and to the relative solvation free energy differences ($\Delta\Delta A_{solv}$) provides a gauge for the convergence of the calculations.

The TI calculations in the gas phase employed Langevin dynamics with a friction coefficient of 60 ps^{-1} and a time step of 1 fs. Random forces were applied according to the target temperature of 300 K. The simulations in solution were carried out under periodic boundary conditions using a truncated octahedron with side length 9.737 Å (V = 10 443.4 $Å^3$). In all simulations there were 348 TIP3P[25] water molecules present. The temperature of the system was kept around 300 K by a Nosé−Hoover thermostat;[26] as in the gas phase the time step was 1 fs. All bonds involving hydrogens were constrained to their equilibrium value by the use of SHAKE,[27] except the two bonds of the CH_2 group in BP (and the bonds to the corresponding dummy atoms; see below). The masses of these two hydrogens were set to 10 amu to avoid convergence problems in the integrator. The Lennard-Jones (LJ) interactions were smoothly switched off between 8 and 9 Å; the electrostatic interactions were calculated with the particle mesh Ewald method,[28] using a 24 × 24 × 24 grid and a damping factor $\kappa = 0.625$ $Å^{-1}$.

The otherwise straightforward alchemical transformations between PP, BP, and F_2BP necessitated dummy atoms as placeholders for the two "disappearing" fluorine/hydrogens atoms at the PP endpoint during the transformations F_2BP ↔ PP and BP ↔ PP. The dummy atoms DF/DH did not participate in any nonbonded interactions. van der Waals endpoint problems were avoided by the use of soft core potentials.[29,30]

(25) Jorgensen, W. L.; Chandrasekhar, J.; Madura, J. D. *J. Chem. Phys.* **1983**, *79*, 926−935.
(26) Hoover, W. G. *Phys. Rev.* **1985**, *A31*, 1695−1697.
(27) Ryckaert, J. P.; Ciccotti, G.; Berendsen, H. J. C. *J. Comput. Phys.* **1977**, *23*, 327−341.
(28) Essman, U.; Perera, L.; Berkowitz, M. L.; Darden, T.; Lee, H.; Pedersen, L. *J. Chem. Phys.* **1995**, *103*, 8577−8593.
(29) Beutler, T. C.; Mark, A. E.; van Schaik, R. C.; Gerber, P. R.; van Gunsteren, W. F. *Chem. Phys. Lett.* **1994**, *222*, 529−539.
(30) Zacharias, M.; Straatsma, T. P.; McCammon, J. A. *J. Chem. Phys.* **1994**, *100*, 9025−9031.

Table 1. Details of the Free Energy Protocols

	N_{wind}[a]	$N_{equ,0}$[b]	N_{equ}[c]	N_{prod}[d]
gas phase	41	60 000	40 000	40 000
solution	41	40 000	20 000	20 000

[a] Number of TI intervals; $\lambda = 0.00, 0.0125, 0.0375, ..., 0.9625, 0.9875, 1.00$. [b] Number of steps for initial equilibration at $\lambda = 0$ or $\lambda = 1$, respectively. [c] Number of equilibration steps for all other TI intervals. [d] Number of steps used for data accumulation in each TI interval.

The bonded interactions involving DF/DH were those of the respective fluorine or hydrogen atoms that they replaced.[31,32] Because of this, the PP endpoints of the two transformations were different; where necessary we denote this by writing PP^{DF} and PP^{DH}, respectively. The free energy difference between PP^{DF} and PP^{DH} cancels from $\Delta\Delta A_{solv}$,[32] but not from ΔA_{gas} and ΔA_{sol}. Therefore, to close the cycle $F_2BP \rightarrow PP \rightarrow BP \rightarrow F_2BP$ individually in the gas phase and in solution, the $PP^{DF} \rightarrow PP^{DH}$ free energy difference had to be computed as well. The free energy difference of each alchemical transition was computed by five forward and five backward TI calculations. A single forward (backward) free energy simulation in the gas phase consisted of a total of 3.3 million MD steps (3.3 ns). To keep the computational effort of the solution calculations manageable, a somewhat shorter (1.6 ns) but otherwise analogous protocol was used. Details of the free energy calculations are summarized in Table 1.

In the calculations involving the monoanions, a special approach was implemented to deal with the additional hydrogen atom on the phosphate/phosphonate group. The presence of the proton modifies the internal rotation about the X−P1 bond (X = OH, CH, CF, respectively) compared to the dianionic case, and it leads to the additional dihedral angle X−P1−O−H. In monoanionic PP (but for neither BP nor F_2-BP), there were multiple conformational substates about the OH−P1 bond that were sampled too infrequently during standard free energy simulations. This problem was avoided by restraining the CZ−OH−P−O dihedral angle at the PP^{DH} and PP^{DF} endpoints to a single conformational minimum, as is standard practice in such cases.[33,34] The free energy cost of the restraint at the modified PP endpoint was computed in a separate step. This correction was also computed by TI; however, in the MD simulations an (adaptive) umbrella potential[35] was added that ensured free rotation about the dihedral angle CZ−OH−P−O (cf. refs 36 and 37). A detailed description of our approach and a comparison with other methods to avoid problems resulting from conformational substates in alchemical free energy simulations was given elsewhere.[47]

For the dianions, which are of greater biological relevance, several additional properties were computed. To understand the contributions to the solvation free energy differences, we carried out additional free energy simulations between the three physical molecules (PP, BP, and F_2BP) and several chimeric solutes. These chimeras shared properties of two of the physical molecules, e.g., a molecular skeleton corresponding to BP (geometry, LJ parameters) bearing partial charges of F_2BP, and so forth. The free energy simulations in the gas phase and in solution were carried out as described above (in particular, the protocols shown in Table 1 were used); however, the solution free energy differences were obtained from only a single forward and a single backward calculation. We also estimated $\Delta\Delta A_{solv}$ by solving the Poisson−Boltzmann (PB) equation for each solute (PP, BP, F_2BP) on a rectangular grid with a spacing of 0.15 Å. The size of the grid (and hence the number of grid points in each spatial direction) was determined from the size of the solute by adding 6 Å in each spatial direction. The dielectric constant ϵ inside the solute was set to one; outside $\epsilon = 80$ was used. The van der Waals radii were taken from refs 38 and 39. The heats of solution (E_{HoS}) of the three solutes were determined from 500-ps MD simulations of PP, BP, and F_2BP in the gas phase and in solution. These simulations were further used to analyze solute−solvent interactions. In addition to the average solute−solvent interaction energy E_{Solu-H_2O}, we computed the interactions of water with (i) the phosphate group (Phos), with (ii) the phenyl ring (Phe), and with (iii) the bridging group X = CF_2, CH_2, and O, that is, the mutation site. These trajectories were also used to compute radial distribution functions (RDF) $g_{X,W}(r)$ between selected atom(s) X of the solute and the oxygen or hydrogen atoms of the waters W; that is,

$$g_{X,W}(r) = \frac{1}{4\pi r^2 \rho} \left\langle \sum_i^{N_{H_2O}} \delta(\mathbf{r} - \mathbf{r}_{iX}) \right\rangle. \quad (3)$$

Finally, to investigate specifics of local solvation, water densities about the solutes were calculated. A three-dimensional grid was constructed about the solute, and a water occupancy histogram was generated. The trajectories were reoriented on the basis of the root-mean-square deviation of the solute coordinates. The count of a bin (an element of the three-dimensional grid) was incremented if in a coordinate frame it was occupied by a water molecule. The raw histogram was converted into the file format used by X-PLOR for electron density maps; these water density maps were displayed using PyMOL.[40]

3. Results

3.1. Parametrization. As part of the present study we developed empirical force field parameters for the pTyr analogues of interest. These supplement the CHARMM22 protein, CHARMM27 nucleic acid, and the fluoroalkane all-atom force fields,[20,21,41] as well as previously published parameters for pTyr.[22] Parameter development was based on the model compounds shown in Figure 1, with both the mono- and dianionic states treated explicitly. Only those parameters unique to the model compounds were optimized in the present work; the remaining parameters were transferred directly from the previously published values. The parameters were developed following published protocols;[42] details of the parametrization are included in the Supporting Information. Briefly, parameter optimization included the adjustment of internal energy terms to reproduce quantum mechanical (QM) geometries and potential energy surfaces for rotations about selected dihedral angles. The partial atomic charges were adjusted to reproduce HF/6-31G* minimum interaction energies and geometries of the model compounds with water. LJ parameters were transferred directly from the CHARMM protein, nucleic acid, and fluoroalkane force fields.[20,21,41] Iterative optimization of the internal parameters following adjustment of the partial atomic charges was performed to ensure that the intra- and intermolecular aspects of the force field were balanced. Figure 1 contains the final set of partial charges; all other parameters are given in Table 3 of the Supporting Information. The parameters may be obtained

(31) Boresch, S.; Karplus, M. *J. Phys. Chem. A* **1999**, *103*, 103−118.
(32) Boresch, S. *Mol. Simul.* **2002**, *28*, 13−37.
(33) Straatsma, T. P.; McCammon, J. A. *J. Chem. Phys.* **1989**, *90*, 3300−3304.
(34) Hermans, J.; Yun, R. H.; Anderson, A. G. *J. Comput. Chem.* **1992**, *13*, 429−442.
(35) Bartels, C.; Karplus, M. *J. Comput. Chem.* **1997**, *18*, 1450−1462.
(36) Tobias, D. J.; Brooks, C. L., III; Fleischman, S. H. *Chem. Phys. Lett.* **1989**, *156*, 256−260.
(37) Straatsma, T. P.; McCammon, J. A. *J. Chem. Phys.* **1994**, *101*, 5032−5039.
(38) Nina, M.; Roux, B. *J. Phys. Chem. B* **1997**, *101*, 5239−5248.
(39) Banavali, N.; Roux, B. *J. Phys. Chem. B* **2002**, *106*, 11026−11035.
(40) DeLano, W. L. *The PyMOL User's Manual*; DeLano Scientific: San Carlos, CA, 2002.
(41) Foloppe, N.; MacKerell, A. D., Jr. *J. Comput. Chem.* **2000**, *21*, 86−104.
(42) MacKerell, A. D., Jr. Atomistic Models and Force Fields. In *Computational Biochemistry and Biophysics*; Becker, O. M., MacKerell, A. D., Jr., Roux, B., Watanabe, M., Eds.; Marcel Dekker: New York, 2001.

Table 2. Results of Alchemical Free Energy Simulations for Dianionic PP, BP, and F_2BP[a]

transition	ΔA_{gas}	ΔA_{sol}	$\Delta\Delta A_{solv}$[b]	$\Delta\Delta A^{PB}_{solv}$	ΔE_{HoS}
$F_2BP \rightarrow PP^{DF}$	−270.38	−279.93	−9.55	−10.7	−10.5
$PP^{DH} \rightarrow BP$	−9.99	−20.27	−10.28	−0.5	−7.4
$BP \rightarrow F_2BP$	280.20	299.99	19.79	11.2	17.9
$PP^{DF} \rightarrow PP^{DH}$[c]	0.19	0.19			
cycle error[d]	0.02	−0.02	−0.04		

[a] In addition to the solvation free energy difference $\Delta\Delta A_{solv}$ for the respective transition, the alchemical gas phase (ΔA_{gas}) and solution free energy differences (ΔA_{sol}) are given. Results of Poisson−Boltzmann calculations ($\Delta\Delta A^{PB}_{solv}$) and relative heats of solution (ΔE_{HoS}) are also presented. All results are in kilocalories per mole. [b] Equation 2. [c] Dummy-atom correction; see the main text for details. [d] Error remaining after closing the cycle $F_2BP \rightarrow PP \rightarrow BP \rightarrow F_2BP$, including the dummy-atom correction where necessary.

Table 3. Results of Alchemical Free Energy Simulations for Monoanionic PP, BP, and F_2BP[a]

transition	ΔA_{gas}	ΔA_{sol}	$\Delta\Delta A_{solv}$[b]
$F_2BP \rightarrow PP^{DF}$	−188.84	−195.24	−6.40
$PP^{DH} \rightarrow BP$	29.23	27.35	−1.88
$BP \rightarrow F_2BP$	159.35	167.88	8.53
$PP^{DF} \rightarrow PP^{DH}$[c]	0.19	0.19	
cycle error[d]	−0.07	0.18	0.25

[a] The alchemical gas phase (ΔA_{gas}) and solution free energy differences (ΔA_{sol}) are given as well. All results are in kilocalories per mole. [b] Equation 2. [c] Dummy-atom correction; see the main text for details. [d] Error remaining after closing the cycle $F_2BP \rightarrow PP \rightarrow BP \rightarrow F_2BP$, including the dummy-atom correction where necessary.

from version 31 of CHARMM, or the reader may access http://www.charmm.org for information on obtaining them. It should be noted that the present optimization procedure was performed to maintain compatibility with the CHARMM protein force field, allowing for application of the parameters in studies of ligand−protein complexes.

3.2. Free Energy Simulations. Overall Results. Tables 2 and 3 contain the results of the free energy simulations for the dianionic and monoanionic forms of the phosphate/phosphonates studied. The precision of the results was very high; for the dianions (Table 2) the highest standard deviation of the individual 10 results (five forward, five backward simulations, cf. section 2) was 0.19 kcal/mol in the gas phase and 0.32 kcal/mol in solution; there was no noticeable hysteresis between the mean of the forward and backward transmutations. In addition, the error for closing the cycle $F_2BP \rightarrow PP \rightarrow BP \rightarrow F_2BP$ was 0.04 kcal/mol for $\Delta\Delta A_{solv}$ and (after taking into account the correction for the two types of dummy atoms) even less for ΔA_{gas} and ΔA_{sol} (last line in Table 2), which is strong evidence that the results are converged. The standard deviations of the results for the monoanionic systems were equally low; the cycle closing error was only slightly higher (0.25 kcal/mol for $\Delta\Delta A_{solv}$, see Table 3). One detail of the results in Tables 2 and 3 requires clarification at this point. All single free energy differences (i.e., the ΔA_{gas} and ΔA_{sol} results) involving F_2BP are extremely large (in the gas phase up to 280 kcal/mol for the dianions, and up to 190 kcal/mol for the monoanions). These numbers are caused by the repulsion between the negative charge of the fluorine atoms and the phosphate oxygens (see Figure 1). However, since this intramolecular effect is present in both parts of the thermodynamic cycle, this contribution mostly cancels from $\Delta\Delta A_{solv}$; the same would be true in binding free energy calculations. The $\Delta\Delta A_{solv}$ results are also depicted graphically

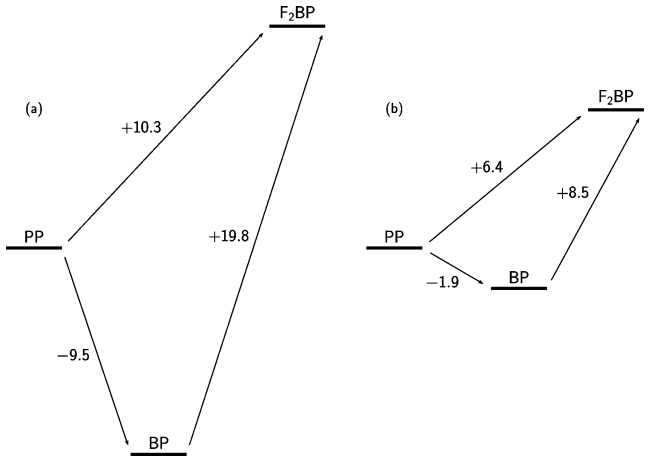

Figure 2. Graphical summary of computed solvation free energy differences $\Delta\Delta A_{solv}$ (in kcal/mol) for (a) dianionic F_2BP^{2-}, BP^{2-} and (b) monoanionic F_2BP^{-}, BP^{-} relative to PP in the respective charge state (cf. Tables 2 and 3).

in Figure 2, which shows the $\Delta\Delta A_{solv}$ results for monoanionic and dianionic BP and F_2BP, respectively, relative to PP. For both the monoanionic and dianionic forms, BP has the lowest free energy of solvation. Similarly, in both ionization states, F_2BP has (by far) the most positive solvation free energy. $\Delta\Delta A_{solv}$ between BP and F_2BP is +19.8 kcal/mol for the dianion and +8.5 kcal/mol for the monoanion.

For the dianions, which are the biochemically more relevant species, additional calculations and analyses were carried out (cf. section 2). The results of PB calculations ($\Delta\Delta A^{PB}_{solv}$, next to last column) and the relative heats of solution ΔE_{HoS} (rightmost column) are listed in Table 2. The agreement of ΔE_{HoS} with the free energy results is excellent and shows that the free energy differences obtained are dominated by enthalpic effects; entropic contributions appear to be negligible. The free energy difference between PP and F_2BP is well-reproduced by continuum electrostatics (+9.6 kcal/mol obtained by TI versus +10.7 kcal/mol obtained by PB). By contrast, the agreement between TI and PB for $\Delta\Delta A^{PP\rightarrow BP}_{solv}$ is poor (−10.3 kcal/mol versus −0.5 kcal/mol). This suggests that local solvation effects not detected by continuum electrostatics play an important role for the transition PP → BP.

Calculations Involving Chimeric Intermediates. To better understand the atomic contributions to the free energy differences, the perturbations were done in steps as described in section 2; such steps include chimeric intermediates that have characteristics of two compounds (e.g., LJ and bond parameters of BP and charges of F_2BP). The free energy differences of solvation involving chimeric intermediates are summarized in Figure 3a for the transition F_2BP to BP and in Figure 3b for F_2BP to PP. In Figure 3 all the paths (i.e., the order in which the intermediate states were traversed) and the corresponding $\Delta\Delta A_{solv}$ results are given. Each step is a free energy difference and does not involve any free energy component analysis, so that the values by themselves are path-independent.[43−45] However, the interpretation of the results is path-dependent. Nevertheless, when validated by careful analysis, experimentally

(43) Mark, A. E.; van Gunsteren, W. *J. Mol. Biol.* **1994**, *240*, 167−176.
(44) Smith, P. E.; van Gunsteren, W. *J. Phys. Chem.* **1994**, *98*, 13735−13740.
(45) Boresch, S.; Archontis, G.; Karplus, M. *Proteins: Struct., Funct., Genet.* **1994**, *20*, 25−33.

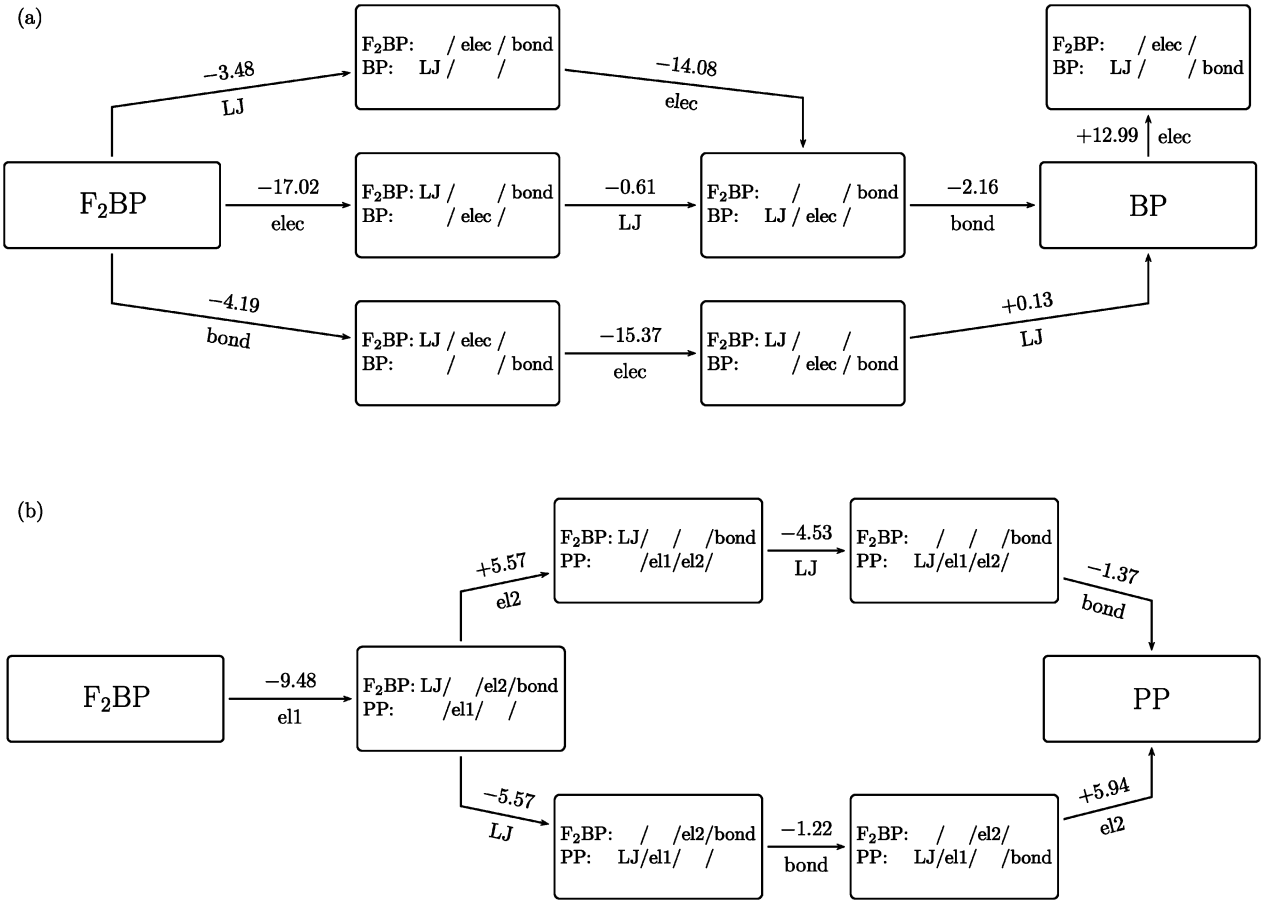

Figure 3. Paths and results of free energy calculations using chimeric intermediate states between (a) $F_2BP \rightarrow BP$ and (b) $F_2BP \rightarrow PP$. All free energies are in kcal/mol.

relevant observations may be obtained from such calculations.[46] Focusing on the largest effect first (i.e., the solvation free energy difference between BP and F_2BP; Figure 3a), we find that the most interesting transitions are those involving chimeras based on BP with F_2BP charges (BP^{q,F_2BP}) and on F_2BP with BP charges ($F_2BP^{q,BP}$). The solvation free energy differences $\Delta\Delta A_{solv}(F_2BP \rightarrow F_2BP^{q,BP})$ and $\Delta\Delta A_{solv}(BP \rightarrow BP^{q,F_2BP})$ are −17.0 and +13.0 kcal/mol, which account for 86 and 66% of $\Delta\Delta A_{solv}^{PP\rightarrow BP}$, respectively. Quite generally, along every pathway (order of alchemical changes) leading from F_2BP to BP the step in which the charges are changed gives the dominant contribution to $\Delta\Delta A_{solv}$. Thus, the major contribution to the overall solvation free energy difference between BP and F_2BP arises from the change in electrostatic interactions between the respective solute and water. Contributions from changes in LJ interactions (i.e., the size difference between the CF_2 and the CH_2 groups) are small. Note that the physical origin of the "bond" contributions in double free energy differences (such as $\Delta\Delta A_{solv}$) is mostly the so-called potential-of-mean-force contribution, that is, the effects caused by the changes in solute geometry (bond lengths, bond angles, etc.) on solute−solvent interactions; cf. refs 31 and 32.

A somewhat different picture emerges for the transition F_2-BP to PP (see Figure 3b). Here, the alchemical changes of charges were done in two steps. First, the fluorine charges were set to zero, and the net charge of the CF_2 group was concentrated on the central carbon atom (transition *el1*). The second transition (*el2*) consisted in changing all remaining charges from the values appropriate for F_2BP to those for PP. These two electrostatic contributions have opposite signs, resulting in a net contribution of only about −4 kcal/mol. The change in LJ parameters contributes about −5 kcal/mol to the overall $\Delta\Delta A_{solv}$. Thus, while the role of electrostatics still is important, the bigger size of the CF_2 group compared with the phosphate ester oxygen becomes significant. $\Delta\Delta A_{solv}^{F_2BP\rightarrow PP}$ consists of almost equal electrostatic and LJ contributions.

Table 4. Decomposition of the Solute−Solvent Interaction Energy into Contributions from the Phosphate Moiety (Phos), the Phenyl Ring (Phe), and the Bridging Group/Atom X, Where X = CF_2, CH_2, and O

transition	ΔE_{X-H_2O}	ΔE_{Phe-H_2O}	ΔE_{Phos-H_2O}	ΔE_{Solu-H_2O}
PP → BP	24.52	−15.37	−26.47	−17.32
PP → F_2BP	5.62	−4.47	13.19	14.34
F_2BP → BP	18.90	−10.90	−39.66	−31.66

[a] The results (in kcal/mole) are given for the energy differences ΔE corresponding to the solvation free energy differences $\Delta\Delta A_{solv}$.

Decomposition of Solute−Water Interactions. The solute−water interaction energy was decomposed into contributions from the phosphate group (Phos), the phenyl ring (Phe), and the bridging group X = CH_2, CH_2, and O, i.e., the modification site. Table 4 presents the results of this decomposition. Instead of giving the absolute values, we report the energy differences corresponding to the free energy differences shown in Table 2.

(46) Boresch, S.; Karplus, M. *J. Mol. Biol.* **1995**, *254*, 801−807.
(47) Leitgeb, M.; Schröder, C.; Boresch, S. *J. Chem. Phys.* **2005**, *122*, 084109.

The respective total difference in interaction energy $\Delta E_{\mathrm{Solu-H_2O}}$ is shown in the rightmost column of Table 4 and is in good qualitative agreement with the corresponding free energy differences of Table 2. BP interacts much more favorably with water than PP (−17.3 kcal/mol); F_2BP, on the other hand, has a much more positive interaction energy (+14.3 kcal/mol) compared with that of PP. For the bridging group X (X = CF_2, CH_2, and O) that is different in the three solutes the transition from PP to BP (O → CH_2) is unfavorable by +24.5 kcal/mol (first entry in the second column in Table 4). Looking at the partial charges of the solutes (Figure 1), one sees that the net charge of the CH_2 group is $q_{CH_2} = -0.1$e, whereas the oxygen in PP bears the negative charge $q_O = -0.28$e. The lower net charge of the CH_2 group compared with that of O certainly is one reason for the unfavorable $\Delta E_{\mathrm{X-H_2O}}$(PP → BP). Further, the CH_2 group is larger than the ester oxygen, and thus the size effect is also expected to be unfavorable. For the transition PP → F_2BP, one also finds a positive change in interaction energy (+5.6 kcal/mol, see second column of Table 4). While the net charge of the CF_2 group ($q_{CF_2} = -0.32$, see Figure 1) is slightly more negative than that of the PP oxygen, CF_2 is certainly much larger, leading to the observed unfavorable change in interaction. This finding agrees with the free energy components obtained from the chimeric intermediates (Figure 3). Looking next at $\Delta E_{\mathrm{Phe-H_2O}}$ (third column in Table 4), one sees that for both phosphonates, BP and F_2BP, the interaction energy is more favorable than that for the phosphate PP (−15.4 and −4.5 kcal/mol, respectively). Since the size of all atoms involved is the same, this difference must be dominated by the charge distribution; indeed, in both phosphonates the partial charges of the phenyl ring are slightly more polar than those in PP (see Figure 1). The third term, the interactions of the phosphate groups with water ($\Delta E_{\mathrm{Phos-H_2O}}$, fourth column in Table 4), makes the largest contribution to $\Delta E_{\mathrm{Solu-H_2O}}$. For PP → BP, $\Delta E_{\mathrm{Phos-H_2O}}$ is highly negative (−26.5 kcal/mol), whereas for PP → F_2BP the interaction is less favorable by +13.2 kcal/mol.

Summarizing the results of our analyses up to this point, two major factors can be discerned: (i) The larger size of the CF_2 group compared to the phosphate ester oxygen leads to poorer solvation of F_2BP compared with PP (and, of course, BP). This is seen both from the interaction energy analysis of Table 4 (positive $\Delta E_{\mathrm{X-H_2O}}$(PP → F_2BP) = 5.6 kcal/mol, despite the more negative net charge of the CF_2 group compared with q_O = −0.28e of PP), as well as by the free energy components obtained from the chimeras (Figure 3). (ii) As reflected by the big free energy difference between BP and F_2BP (+19.8 kcal/mol), which is dominated by electrostatic effects (cf. the free energy "components" obtained by means of the chimeric intermediates, Figure 3a), small changes in charge distribution can have major effects on solvation free energies. Thus, it is quite interesting to take a closer look at the partial charges shown in Figure 1. In all three solutes most of the negative charge is located on the PO_3 group. The replacement of the phosphate ester oxygen by a CH_2 group pushes additional negative charge into the phosphate group ($q^{\mathrm{BP}}_{\mathrm{PO_3}} = -1.49$e versus $q^{\mathrm{PP}}_{\mathrm{PO_3}} = -1.44$e) and into the ring. The electronegative fluorines, on the other hand, attract negative charge and, in particular, lower the net charge of the PO_3 group ($q^{\mathrm{F_2BP}}_{\mathrm{PO_3}} = -1.36$ e). A quick calculation shows that these apparently small changes are significant. Inserting the net charges of the PO_3 group in BP and F_2BP into the Born equation and assuming a radius of 5 Å gives a free energy difference of ∼12 kcal/mol, about 60% of the total free energy difference obtained from simulation.

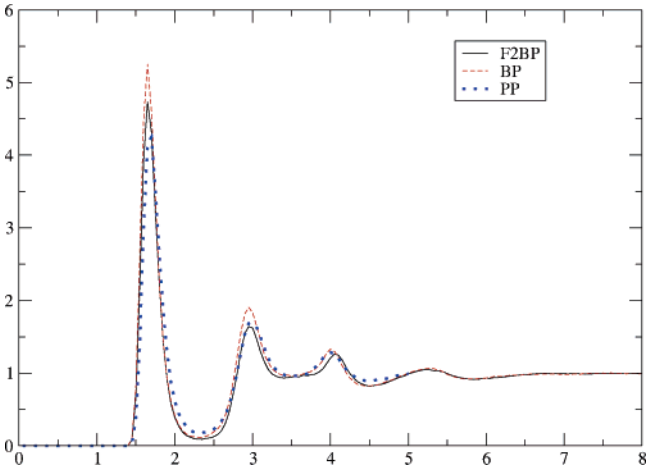

Figure 4. RDF $g_{O_PW_H}(r)$ (eq 3) between phosphate oxygens and water hydrogens for F_2BP, BP, and PP.

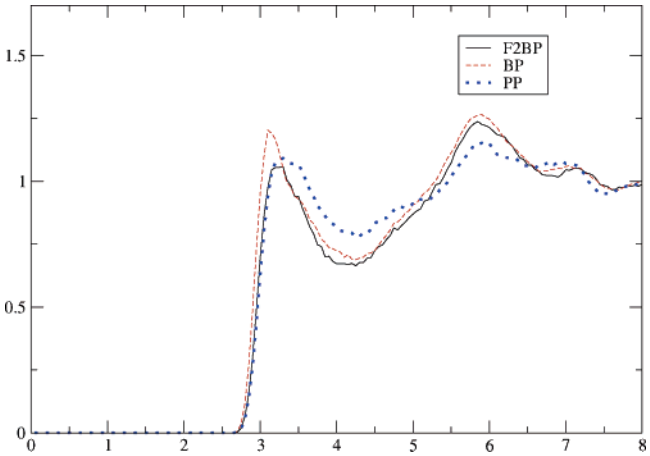

Figure 5. RDF $g_{C_\epsilon W_O}(r)$ (eq 3) between the two C_ϵ atoms of the benzene ring and the water oxygens for F_2BP, BP, and PP.

Local Solvation Structure. The factors just discussed (size differences, changes in charge distribution) should be included in free energy differences of solvation obtained from numerical solutions of the PB equation. The poor results for $\Delta\Delta A^{\mathrm{PP\to BP}}_{\mathrm{solv}}$ (see Table 2), therefore, indicate that there must be some additional contributions that are not accounted for by a continuum electrostatics approach. To obtain a better understanding of the solvation of the three solutes on the molecular level, we looked at several radial distribution functions and local water density maps (cf. section 2). The first RDF studied (Figure 4) shows $g(r)$ between the three PO_3 oxygens and the water hydrogens for F_2BP (solid line), BP (dashed line), and PP (dotted line). Aside from the small difference in height of the first peak, the three functions are remarkably alike. Larger differences between the three solutes are visible in the RDFs between the two C_ϵ carbons of the benzene ring (averaged over both carbons) and the water oxygens, which are shown in Figure 5. PP is characterized by a first minimum and second maximum that are somewhat shallower compared with those of BP and F_2BP. Most importantly, the first maximum of PP is noticeably lower than that of BP and located further out as well. F_2BP has the lowest maximum of all three compounds. Substantial differences

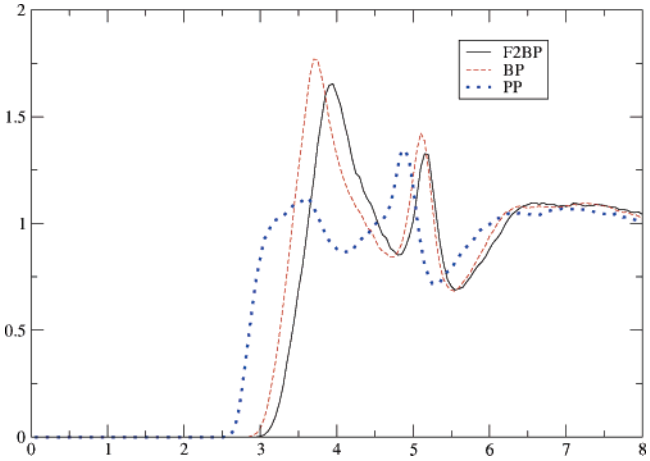

Figure 6. RDF $g_{XW_O}(r)$ (eq 3) between the atoms X = CF (F_2BP), CH (BP), and OH (PP) and the water oxygens.

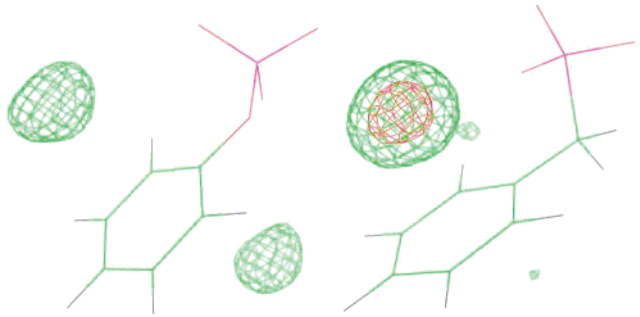

Figure 7. Water density maps (cf. section 2) for PP (left) and BP (right). Green: 70% isodensity surface. Red: 80% isodensity surface.

are also visible in the $g(r)$ between the carbon of the CH_2 and the CF_2 group in BP and F_2BP, respectively, and the oxygen atoms of the solvent waters, which we compare to the $g(r)$ between the ester oxygen in PP and the water oxygens (Figure 6). The PP RDF (dotted line) has a broad but very low first minimum starting at about 2.6 Å, whereas the RDFs of BP (dashed line) and F_2BP (solid line) both start further out at approximately 3 Å. This is, of course, expected because of the smaller size of the ester oxygen compared with the CH_2/CF_2 moieties. The shallowness of the first peak in the RDF of PP, however, indicates that the ester oxygen has no distinct first solvation shell compared to the CH_2/CF_2 groups of BP and F_2-BP, respectively. The difference in size of the methylene (BP) and difluoromethylene groups (F_2BP) is reflected in the position of the first maximum, which lies about 0.2 Å further out for F_2BP; the BP maximum is also noticeably higher.

While the different net charges of the PO_3 moieties are reflected only weakly in the corresponding RDF $g_{O_PW_H}(r)$ (Figure 4), the analysis of the RDFs, nevertheless, reveals interesting differences between PP and BP. Both the C_ϵ ring carbon atoms (Figure 5), as well as the bridging group (Figure 6) in BP, are more strongly coordinated by water compared with PP. The origin of these differences can be rationalized with the help of the water density maps shown in Figure 7. PP is shown on the left, BP on the right. The green isodensity surface corresponds to a 70% probability that a water molecule is found within the particular volume element at any given time. (An 80% probability—red isosurface—can only be discerned in BP.) In PP equal water density is seen on both sides of the aromatic ring. By contrast, the water density around BP is highly asymmetric; while there is practically no density on one side of the aromatic ring, much more and higher density is seen on the opposite side. The different behavior results from subtle differences in conformation. As shown in Figure 7, PP has a low energy conformation with essentially C_{2v} symmetry (i.e., the aromatic ring, the ester oxygen and the phosphorus atom lie in one plane). In BP (and F_2BP), this symmetry is broken since the PO_3 group is pushed out of the ring plane for steric reasons. The bent conformation of BP positions the PO_3 group and the ring similar to the two jaws of a pair of pliers that can tightly coordinate water. The one-sided but much higher density found in BP compared with PP is the consequence. While the pictures shown in Figure 7 were obtained by fitting to the respective gas-phase minimum energy structures, two-dimensional potential-of-mean-force maps with respect to the relevant dihedral angles show that these conformations are also low-lying energy minima in solution (data not shown). The minima in the CE1−CZ−CH−P1 dihedral angle in BP (double-well like minima at −115°/−65° and +65°/+115°) are systematically displaced compared to the corresponding minima in the CE1−CZ−OH−P1 dihedral angle of PP (flat, wide minima at 0°, 180°), so the observed differences between BP and PP remain regardless of the particular conformational minimum populated by the system. The differences in the water densities agree with the higher degree of correlation seen for BP compared with PP in some of the RDFs, in particular the RDFs involving the C_ϵ ring carbon atoms (Figure 5), as well as the bridging group (Figure 6).

Analogous considerations apply in principle to F_2BP as well, which also adopts a bent conformation quite similar to that of BP. However, any favorable contribution for F_2BP that might result from changes in local solvation is more than offset by the change in charge distribution, as reflected by the free energy components obtained from the chimeric intermediates (Figure 3a). This is also seen from the RDFs, where for F_2BP the interactions with water are always weaker than those of BP. As compared with PP the larger size of the CF_2 group is also unfavorable.

4. Discussion

The development of force field parameters for (fluorinated) methyl phosphonates is an important step toward a better understanding of binding to and inhibition of proteins relevant to pTyr-dependent signal transduction. The first application of the new parameters presented here, the calculation of the relative free energy differences of solvation for the side chain analogues PP, BP, and F_2BP, complements experimental attempts to rationalize the binding affinities of peptides containing pTyr, Pmp, and F_2Pmp. The present results show the phosphonate BP to be the most favorably solvated, whereas the fluorophosphonate is solvated least well, with the total differences being 19.8 and 8.5 kcal/mol for the di- and monoanionic species, respectively. To date, analysis of the observed binding affinity differences has focused on the interactions between the protein and ligand/inhibitor; the significant differences in solvation free energies are a novel fact that needs to be taken into account when interpreting the binding data.

Consistent with the obtained relative free energies of solvation, the cost of desolvation is highest for BP (hence Pmp) and

lowest for F_2BP (hence F_2Pmp) upon binding to the pTyr binding pocket of a protein. These results indicate that binding of the fluorophosphonate moiety should be favored over Pmp (and pTyr) because of its less negative solvation free energy. In fact, on the basis of solvation considerations alone and assuming full desolvation of the inhibitors,[17] binding of the F_2-BP versus the BP analogues will be favored by a factor of 10^6 for the monoanionic species and 10^{14} for the dianionic species! In comparison, the experimentally determined binding potencies of F_2Pmp- versus Pmp-containing peptides range from slightly poorer for certain SH2 domains[16] to a 1000-fold increase for PTP1.[12,13] Such differences suggest that the direct binding strength of F_2Pmp for the proteins (i.e., ignoring solvation considerations) may be actually less than that of Pmp.

An important difference that needs to be addressed is the p$K_{a,2}$ values for the three amino acids (pTyr, Pmp, F_2Pmp). At pH 7, pTyr and F_2Pmp, with p$K_{a,2}$ values of 5.7 and 5.1, respectively, are essentially dianionic; however, both ionization states are present for Pmp (p$K_{a,2}$ = 7.1).[12] Thus, the presence of a significant amount of the Pmp monoanion at physiological conditions, which has a significantly less favorable free energy of solvation as compared to the dianion, would further favor the binding affinity on the basis of the solvation arguments given above. Furthermore, the ordering of the solvation free energies, BP < PP < F_2BP, is the same in both charge states. However, experimentally it is observed that pH has no influence on the inhibitory potency of Pmp and F_2Pmp,[12] suggesting that for the binding process only the dianionic form is relevant. Thus, while an impact of ionization state on the arguments made presently cannot be totally excluded, it is clear that it will not alter the conclusions being made.

The molecular origin of the differences in solvation free energies is due to a combination of effects. The solvation free energy of the molecular ions is quite sensitive to small changes in charge distribution. While the electronegative fluorines attract negative charge and, thus, smear it over the full molecule and, in particular, reduce the charge density on the PO_3 group, the apolar CH_2 moiety of BP pushes negative charge into the PO_3 group. The significant increase in size of the CF_2 group relative to the methylene group of BP and the ester oxygen of PP further lowers the aqueous solubility of F_2BP. The origin of $\Delta\Delta A_{solv}^{PP\rightarrow BP}$ lies in subtle differences of local solvation of the phosphate and the phosphonate, caused by differences in conformation about the CE1−CZ−X−P dihedral angle.

While the experimental data for the binding of pTyr, F_2Pmp, and Pmp to SH2 domains and PTP1 obviously include significant influences from direct interactions with the binding site, the analysis of the molecular origin of the solvation free energy differences may provide some hints on the determinants of the selectivity. One factor contributing to the poorer solvation of the fluorophosphonate is the size of the CF_2 moiety. In small, narrow binding pockets fluorination may thus have little effect or even be detrimental for steric reasons, whereas in spacious binding sites, where the bigger size of F_2Pmp is of no consequence, it may lead to better binding because of the lowered desolvation penalty. Second, because of the observed large effects on the solvation free energy resulting from small differences in charge distribution of the solutes, it is reasonable to expect that direct binding interactions between protein and ligand (inhibitor) will also be influenced strongly by the details of the complementary charge distribution in the respective binding pocket. Binding affinities may also depend on whether size and shape of the binding pocket can accommodate the conformational differences between the phosphate group and the phosphonates, which could be shown to be relevant for the observed solvation free energy difference between BP and PP. Finally, while the solvation free energy of F_2BP is less negative than that of BP and PP, its polarity and capability to form hydrogen bonds remain intact.[21] In fact, the dipole moment of F_2BP (using the phosphorus as the origin of the coordinate system) is higher than that of PP and BP. In their detailed study why F_2Pmp is a more potent inhibitor than Pmp, Chen et al. suggested that the "two fluorine atoms restore or enhance the hydrogen-bonding interactions normally between the phenolic oxygen in pTyr and side chains in the active site of PTP1".[12] In other words, the CF_2 group is a non-hydrolyzable replacement for the ester oxygen of pTyr, which closely mimics its capabilities to interact with atoms of the receptor protein. Reducing the hydrophilicity of a solute while retaining its polarity may well be a general principle explaining the efficacy of selective fluorination, as previously discussed.[21]

The parameter optimization for Pmp and F_2Pmp and the calculation and analysis of solvation free energy differences between the side chain analogues PP, BP, and F_2BP are but a first step toward a better understanding of the factors determining binding affinity and selectivity toward PTPs and SH2 domains. The availability of parameters for PP,[22] BP, and F_2-BP and, hence, for pTyr, Pmp, and F_2Pmp provides the basis for detailed computational studies of PTPs and SH2 domains complexed with both their natural ligand as well as an important class of inhibitors.

Acknowledgment. This work was supported by Grant P-16361-B07 of the Austrian FWF to S.B. and by NIH Grants GM51501 and CA95200 and the University of Maryland School of Pharmacy Computer-Aided Drug Design Center to A.D.M. We thank Terrence Burke for helpful advice, Tibor Rudas for practical help with some of the calculations, and Tom Woolf for suggesting the use of water density maps as a tool to explore local solvation phenomena. S.B. acknowledges numerous helpful discussions with Othmar Steinhauser.

Supporting Information Available: Details of the parameter optimization approach and a complete parameter listing (PDF). This material is available free of charge via the Internet at http://pubs.acs.org.

JA044935H